Atmospheric Chemistry and Physics Open Access

Supplement of Atmos. Chem. Phys., 16, 3761–3812, 2016
http://www.atmos-chem-phys.net/16/3761/2016/
doi:10.5194/acp-16-3761-2016-supplement

Supplement of

Ice melt, sea level rise and superstorms: evidence from paleoclimate data, climate modeling, and modern observations that 2 °C global warming could be dangerous

James Hansen et al.

Correspondence to: James Hansen (jeh1@columbia.edu)

Supplement S1: Figures S1-S24, and Supplements S2 and S3 with Photograph S1

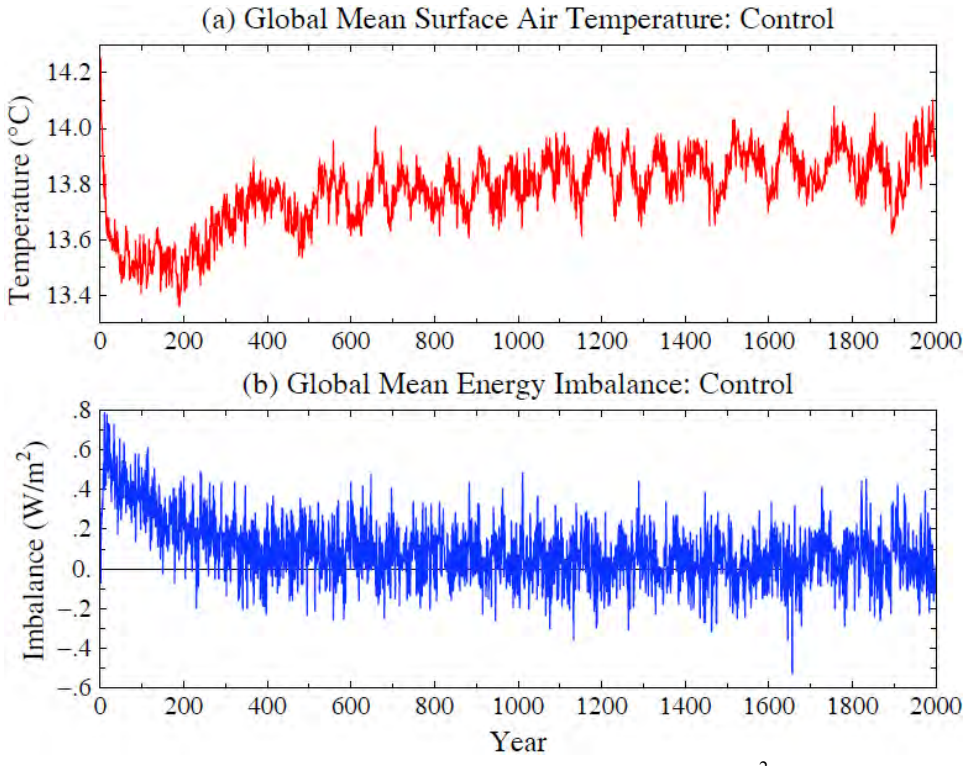

Fig. S1. Surface air temperature (°C) and planetary energy imbalance (W/m^2) in the control run.

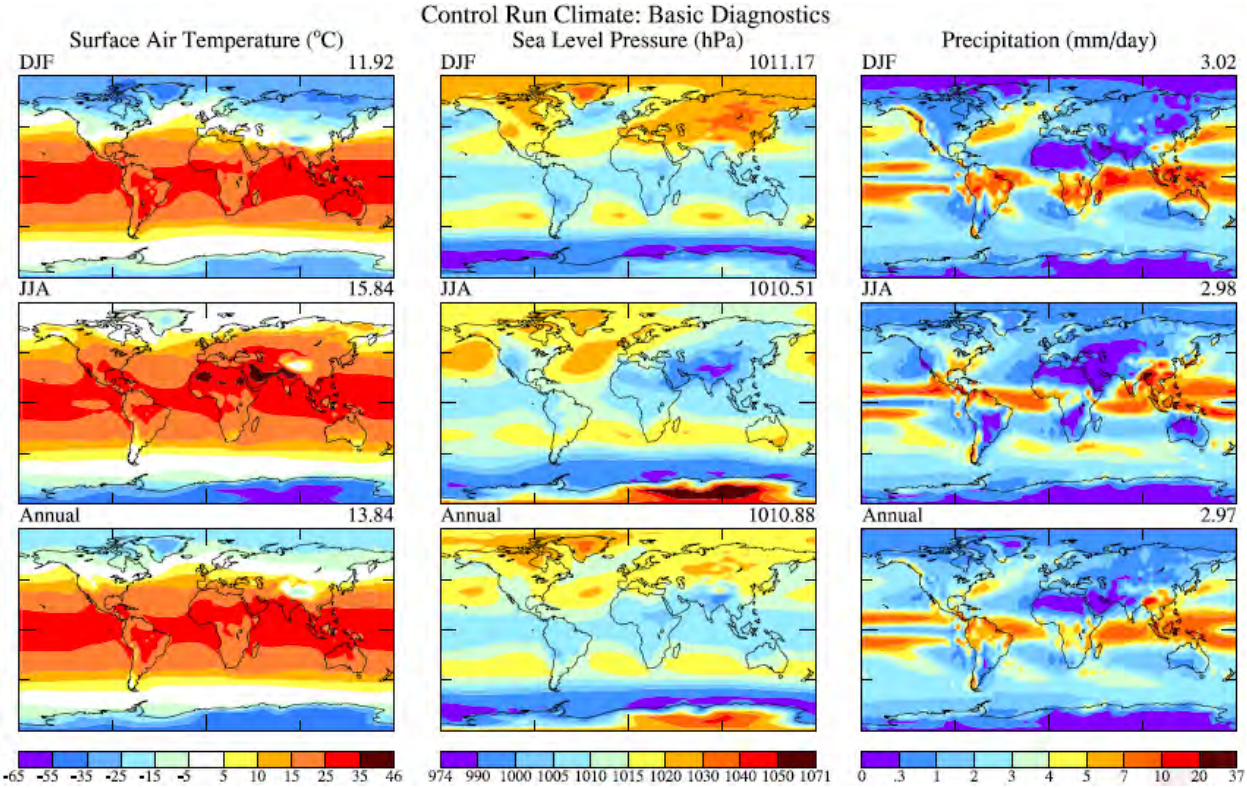

Fig. S2. Surface air temperature (°C), sea level pressure (hPa) and precipitation (mm/day) in Dec-Jan-Feb (upper row), JJA (middle row) and annual mean (lower row) in the climate model control run.

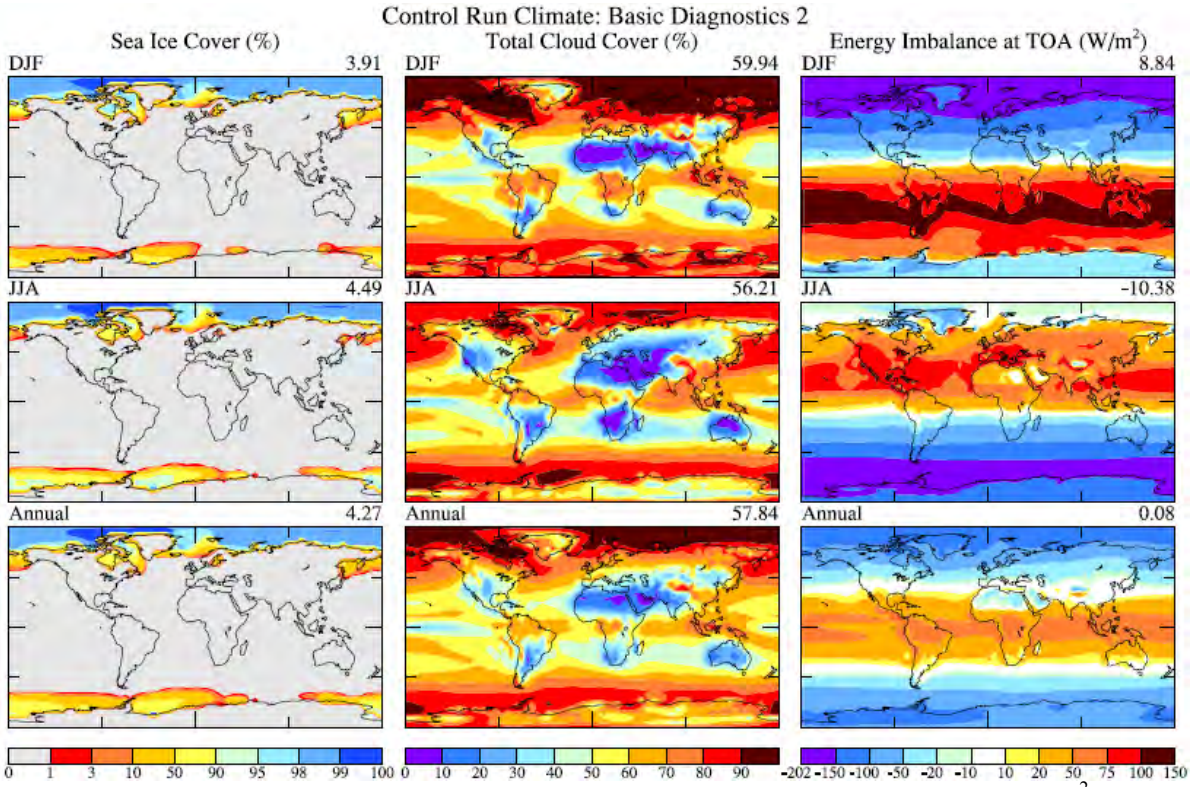

Fig. S3. Sea ice cover (%), cloud cover (%) and top of atmosphere energy imbalance (W/m^2) in Dec-Jan-Feb (upper row), JJA (middle row) and annual mean (lower row) in climate model control run.

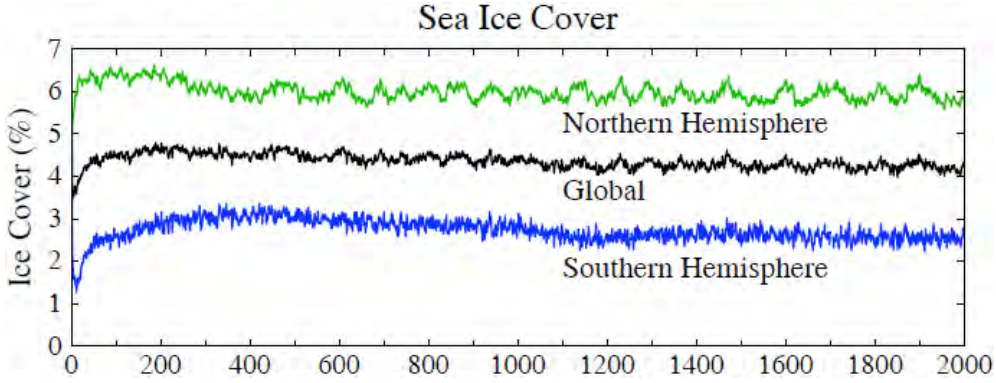

Fig. S4. Hemispheric and global sea ice cover (%) versus time in the control run.

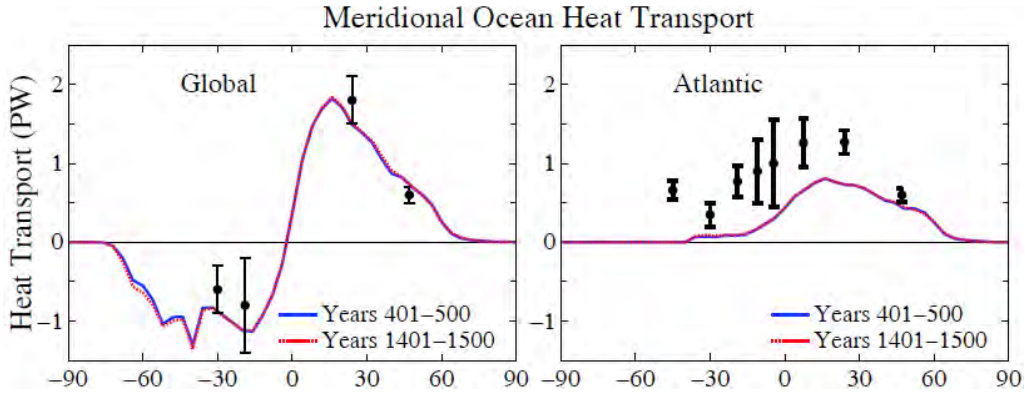

Fig. S5. Poleward transport of heat (PW) by the ocean in 5th and 15th centuries of the control run. Observational estimates (black dots with error bars) are from Ganachaud and Wunsch (2003).

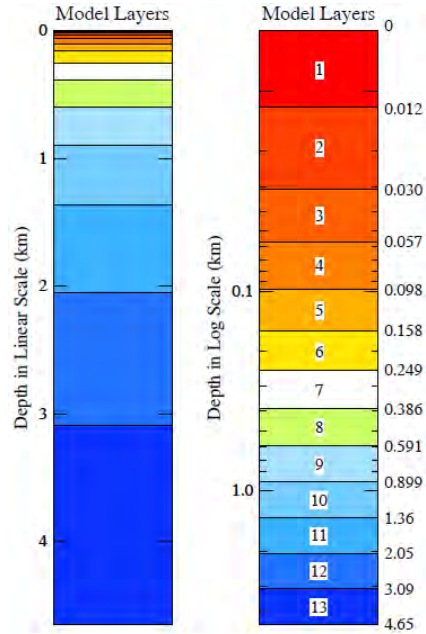

Fig. S6. Layer depths in ocean model.

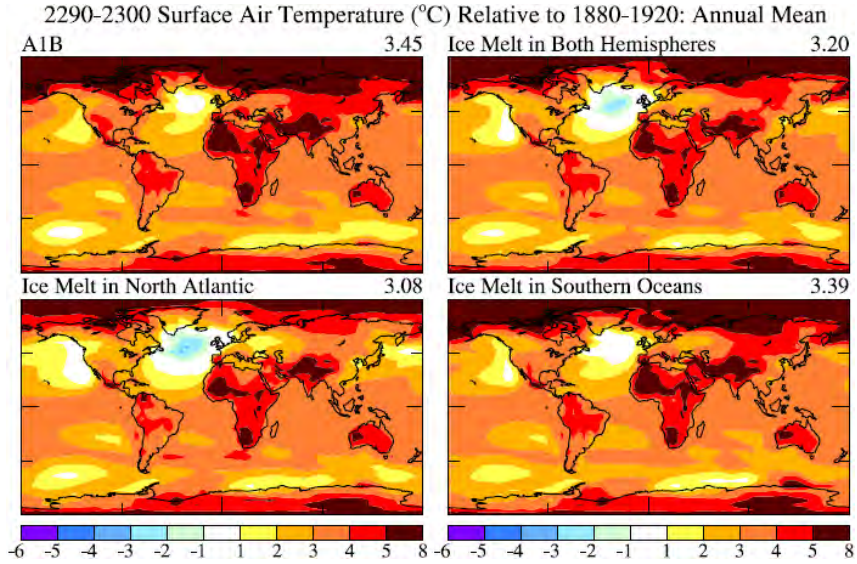

Fig. S7. Surface air temperature change (°C) relative to 1880-1920 in 2290-2300 for the four climate forcing scenarios shown in Fig. 8.

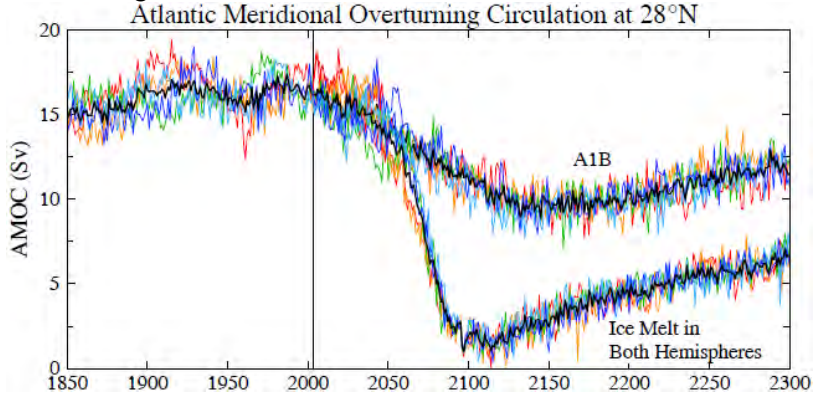

Fig. S8. AMOC strength (Sv) at 28N in five ensemble members and their mean (heavy black line) for the A1B GHG scenario and for that scenario plus ice melt in both hemispheres with 10-year doubling time reaching a maximum 5 m contribution to sea level.

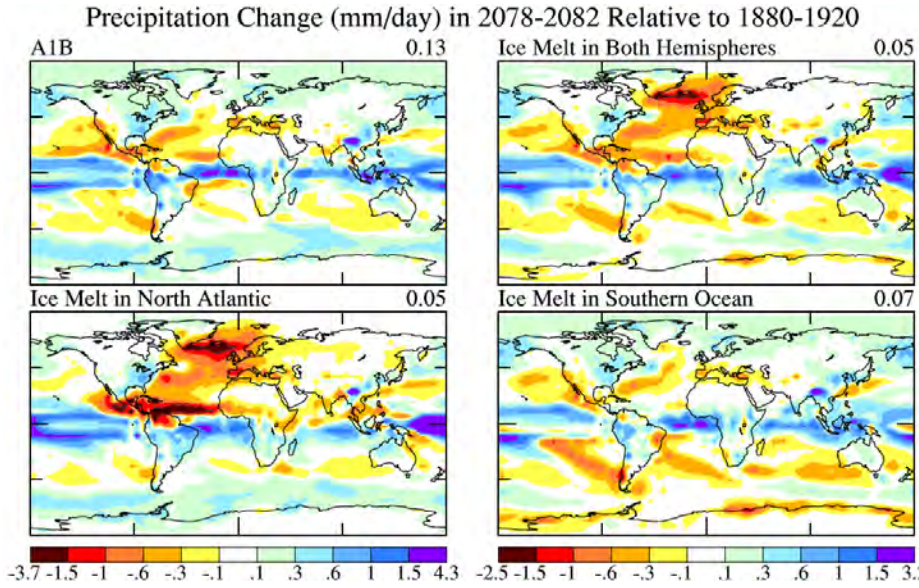

Fig. S9. Precipitation change (mm/day) in 2078-2082 for the same four scenarios as in Figs. 6 and 8.

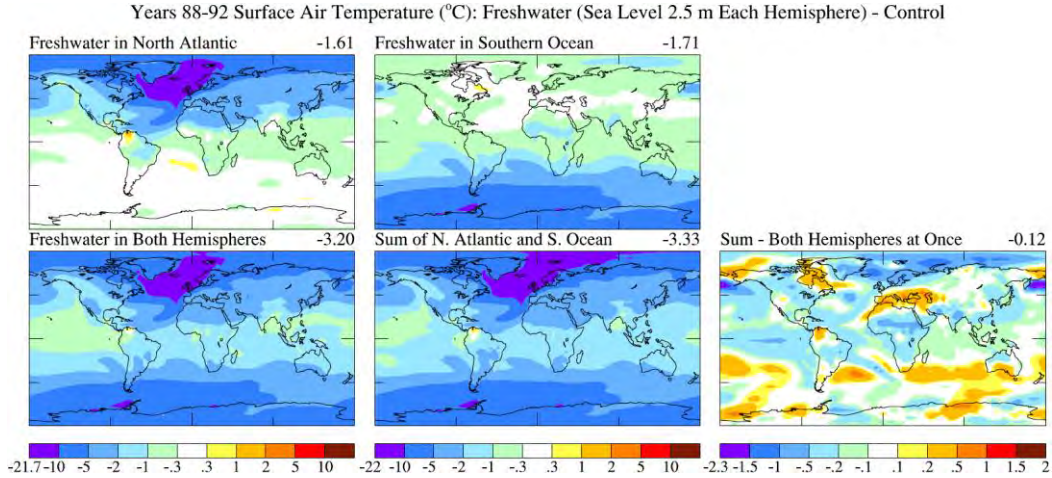

Fig. S10. Surface air temperature change (°C) in pure freshwater experiments at time of peak cooling (years 88-92) in three experiments with 2.5 m freshwater in each hemisphere. The sum of responses to the hemispheric forcings is compared with the response to forcing in both hemispheres in the bottom row.

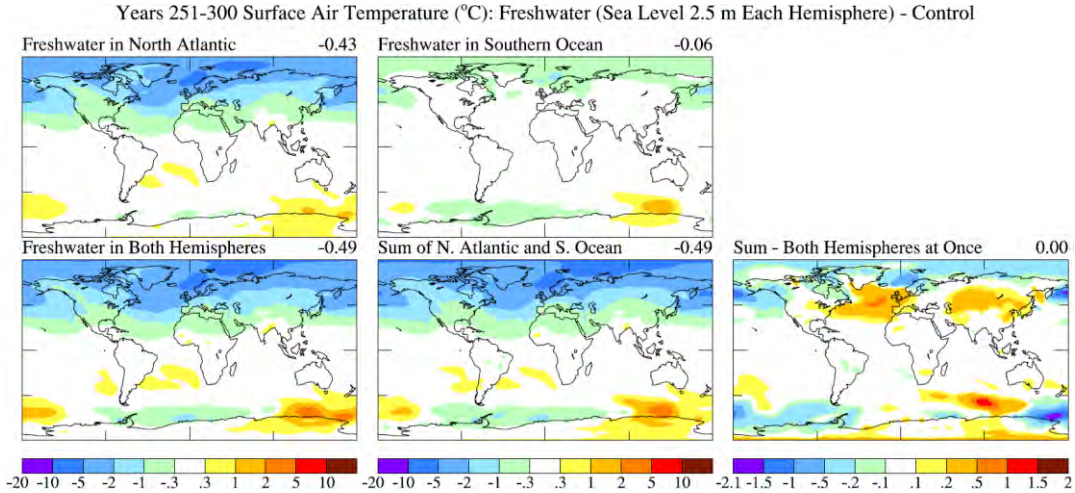

Fig. S11. Same as Fig. S10, but for years 251-300.

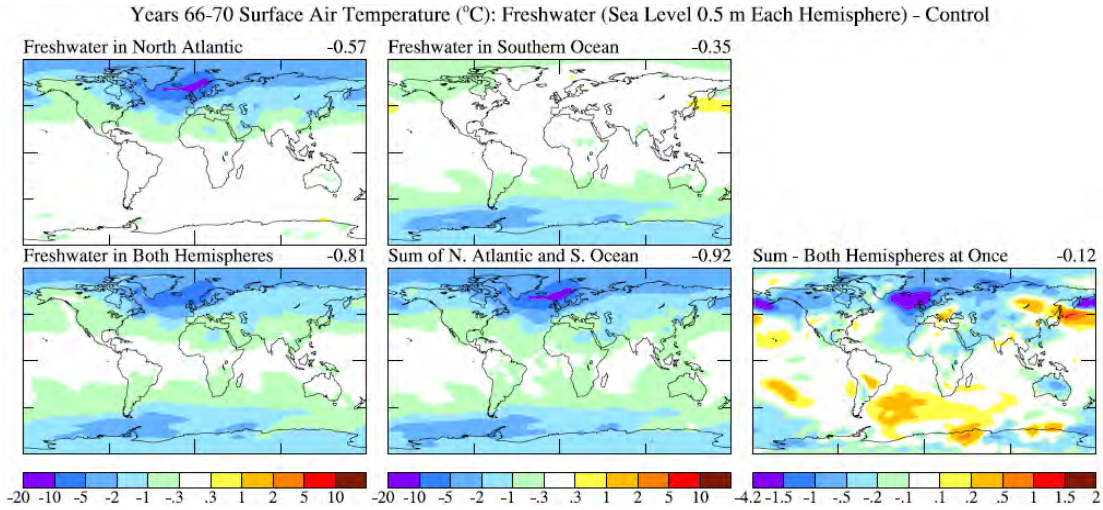

Fig. S12. Same as Fig. S10, but for hemispheric freshwater inputs of 0.5 m at years 66-70.

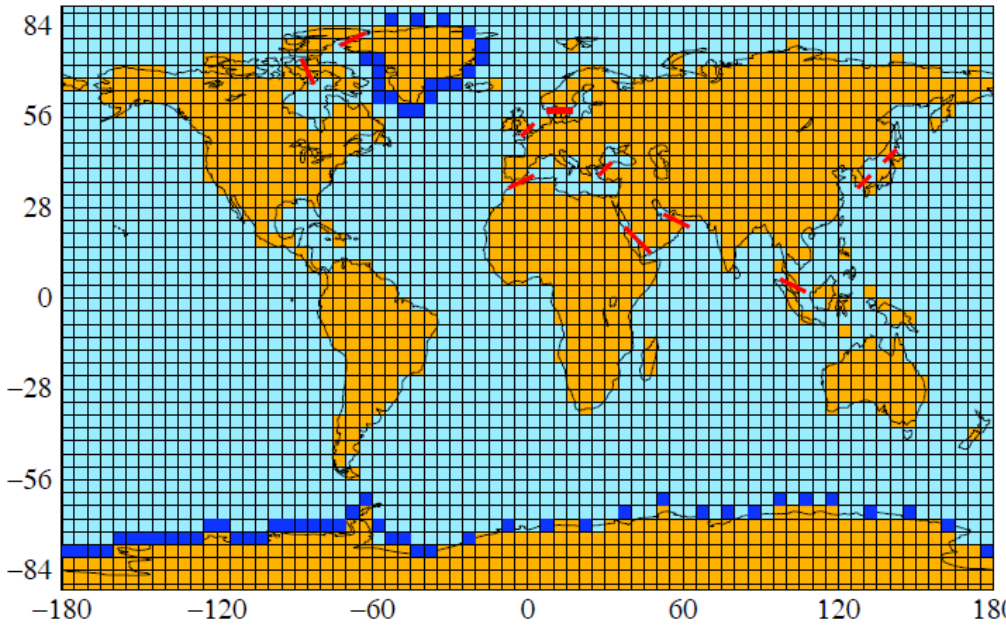

Fig. S13. Climate model grid. Dark blue gridoxes are locations of freshwater insertion. Red lines mark the 12 straights connecting ocean gridboxes.

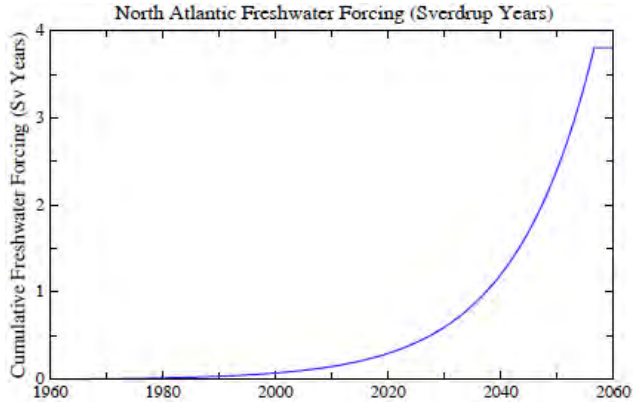

Fig. S14. Freshwater forcing (Sv years) in the North Atlantic in modified forcings scenario, i.e., the runs that have 360 Gt freshwater injection in 2011 with freshwater at earlier and later times based on 10-year doubling. Freshwater injection onto the Southern Ocean is double the North Atlantic rate.

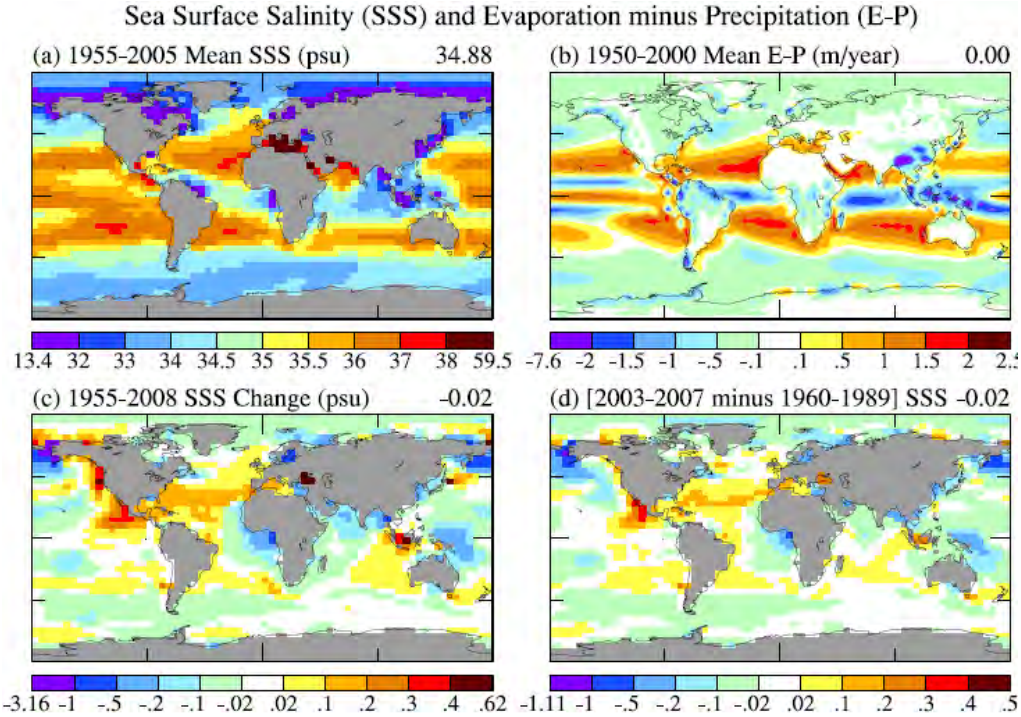

Fig. S15. (a) Simulated sea surface salinity (psu), (b) evaporation minus precipitation (m/yr), and (c,d) salinity change (m/yr), periods being chosen to allow comparison with observations, as discussed in text.

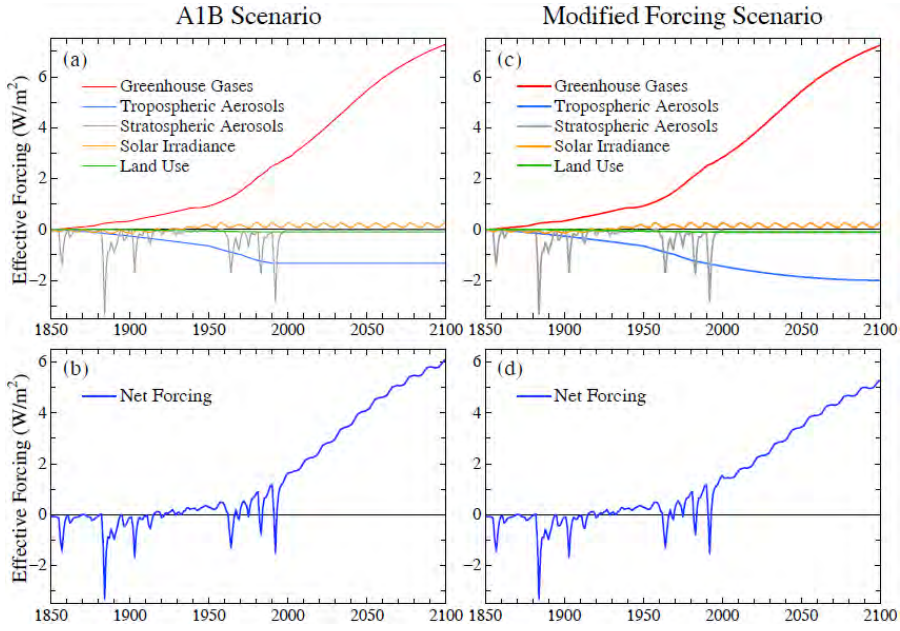

Fig. S16. Effective global climate forcings (W/m^2) in our climate simulations relative to values in 1850.

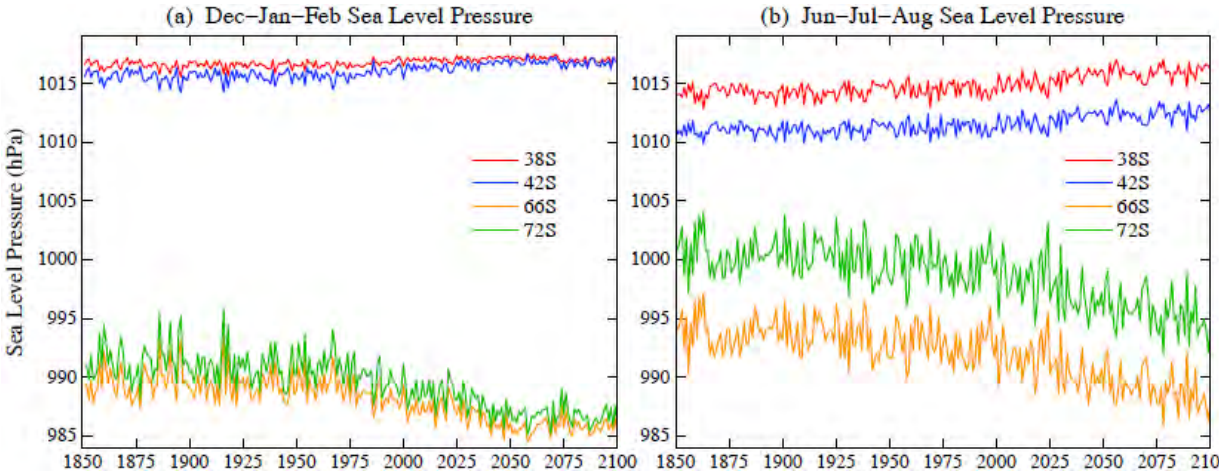

Fig. S17. Sea level pressure (hPa) at four latitudes in (a) Dec-Jan-Feb and (b) Jun-Jul-Aug. Model is driven by "modified" forcings including ice melt reaching the equivalent of 1 m sea level by mid-century.

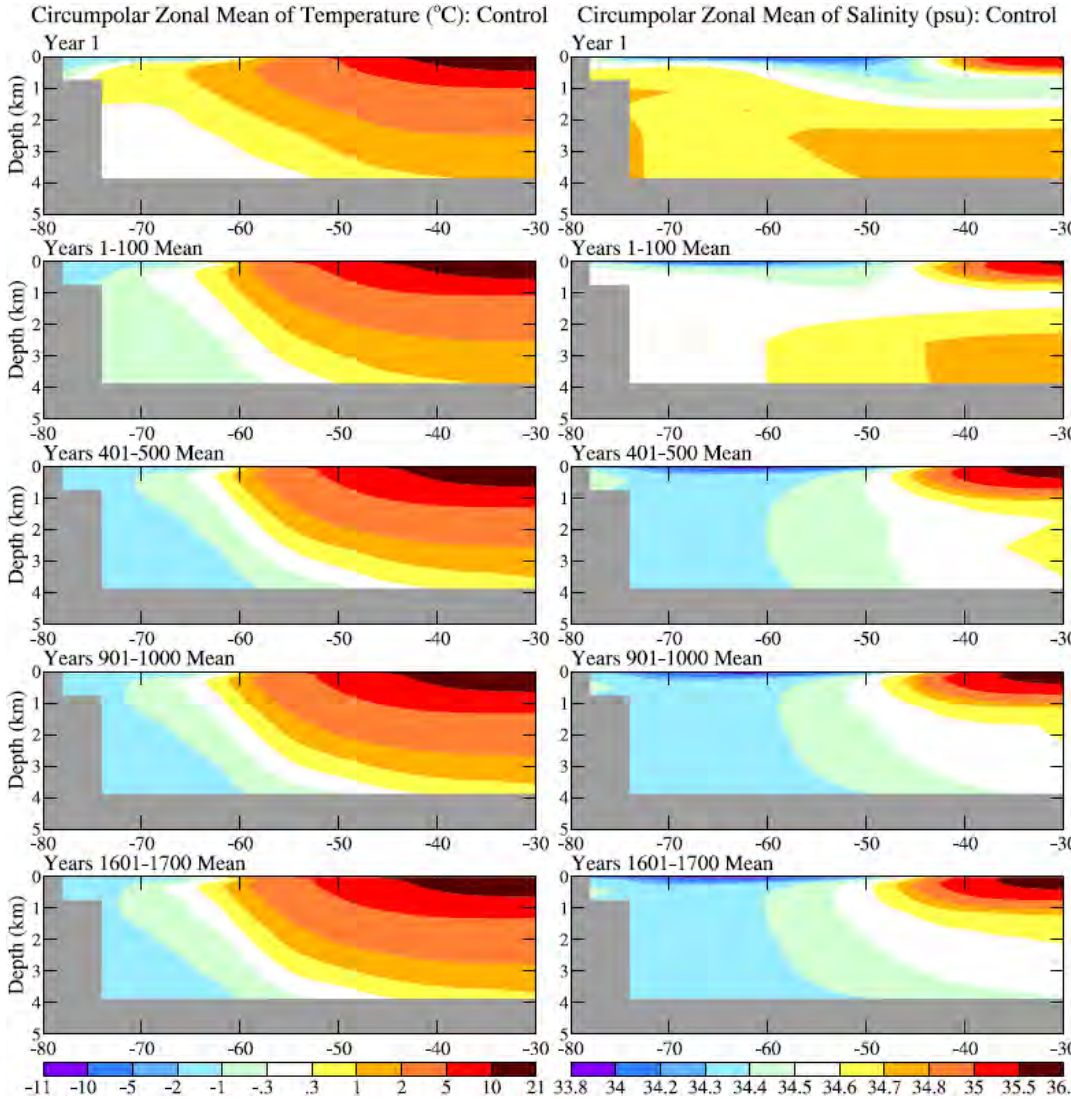

Fig. S18. Ocean temperature (°C) and salinity (psu) in the control run.

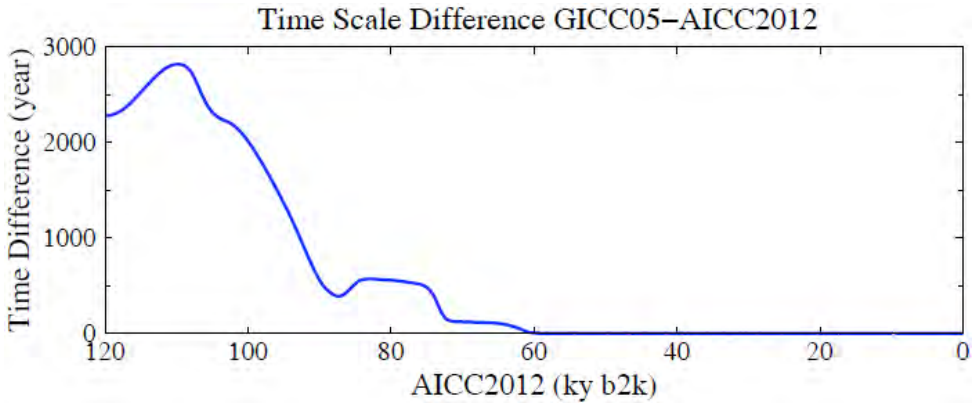

Fig. S19. Difference (years) between the GICC2005modelext and AICC2012 time scales (Bazin et al., 2013; Veres et al., 2013; Rasmussen et al., 2014; Seierstad et al., 2014).

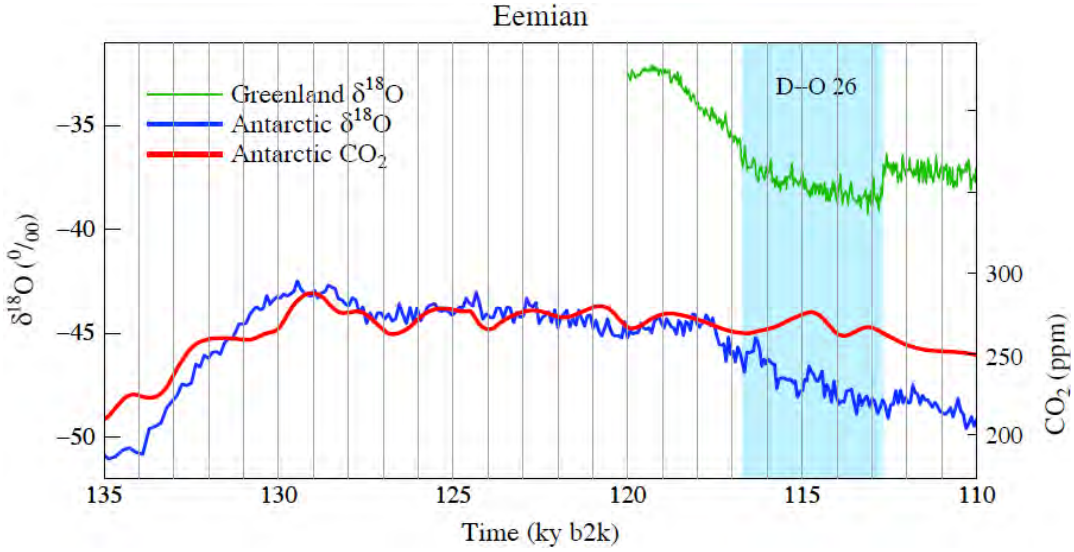

Fig. S20. Expansion of data from Fig. 27b,c. CO_2 increases during D-O 26 lag Antarctic temperature rises by 1500-2000 years.

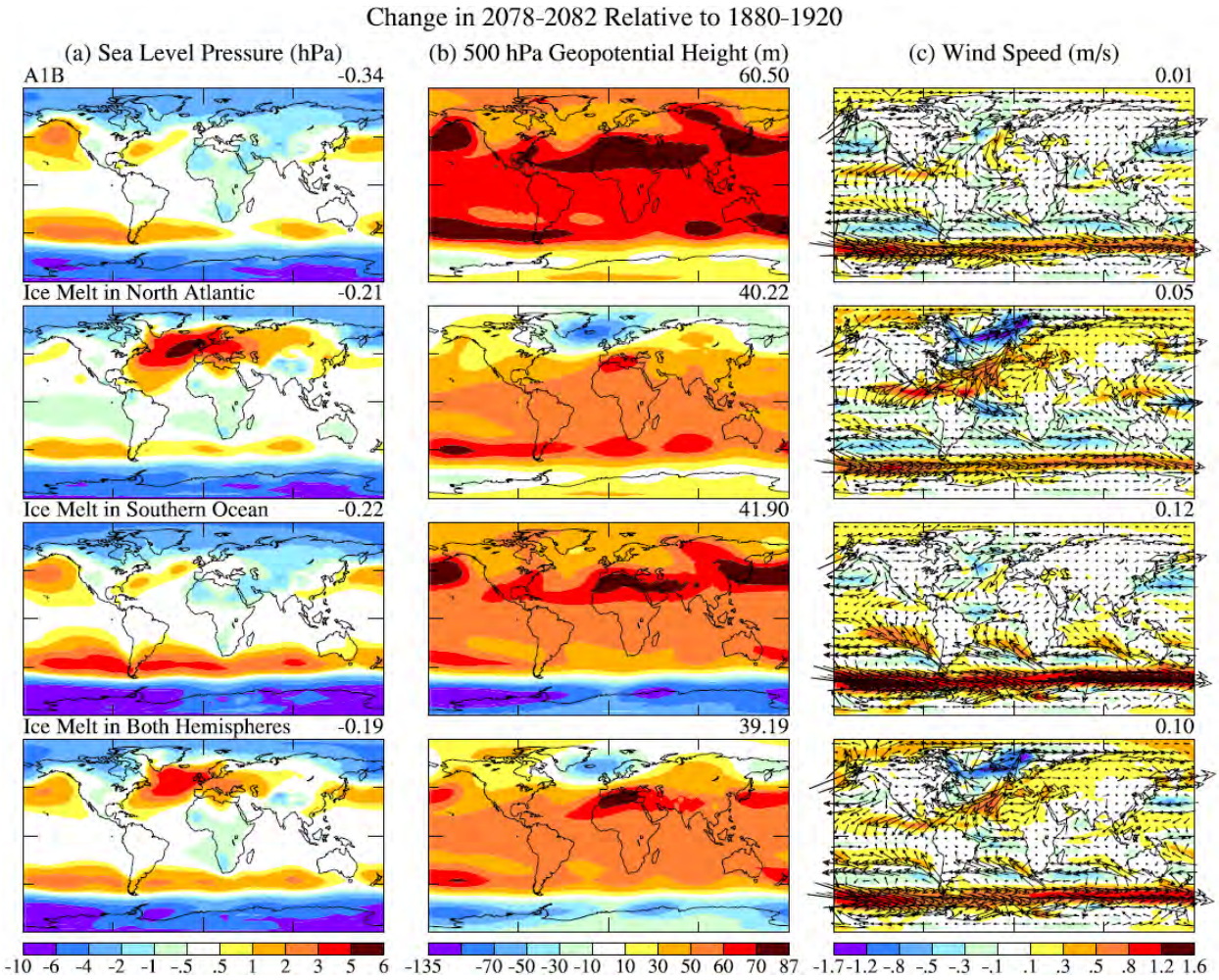

Fig. S21. Change in 2078-2082, relative to 1880-1920, of the annual mean **(a)** sea level pressure (hPa), **(b)** 500 hPa geopotential height (m), and **(c)** wind speed (m/s), for the same four scenarios as in Fig. 6. Numbers in upper right corners are the global mean change.

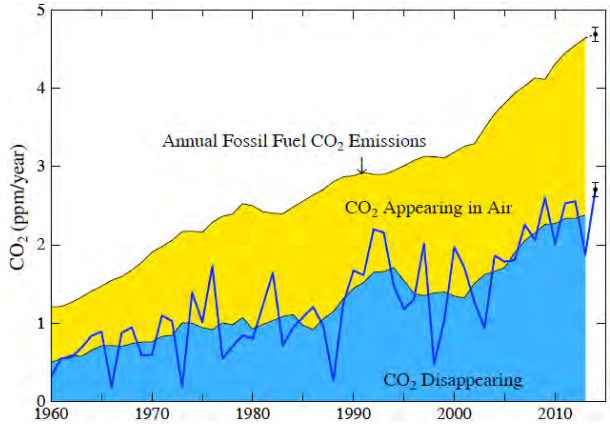

Fig. S22. Top curve: global fossil fuel CO_2 emissions (ppm/year). Measured CO_2 increase in air is the yellow area. The 7-year mean of CO_2 being absorbed by the ocean, soil and biosphere is blue (5- and 3-year means at the end; dark blue line is annual). 2014 global emissions estimate as 101% ±2% of 2013 emissions. CO_2 emissions from Boden et al. (2013) and atmospheric CO_2 from P. Tans (www.esrl.noaa.gov/gmd/ccgg/trends) and R. Keeling (www.scrippsco2.ucsd.edu/).

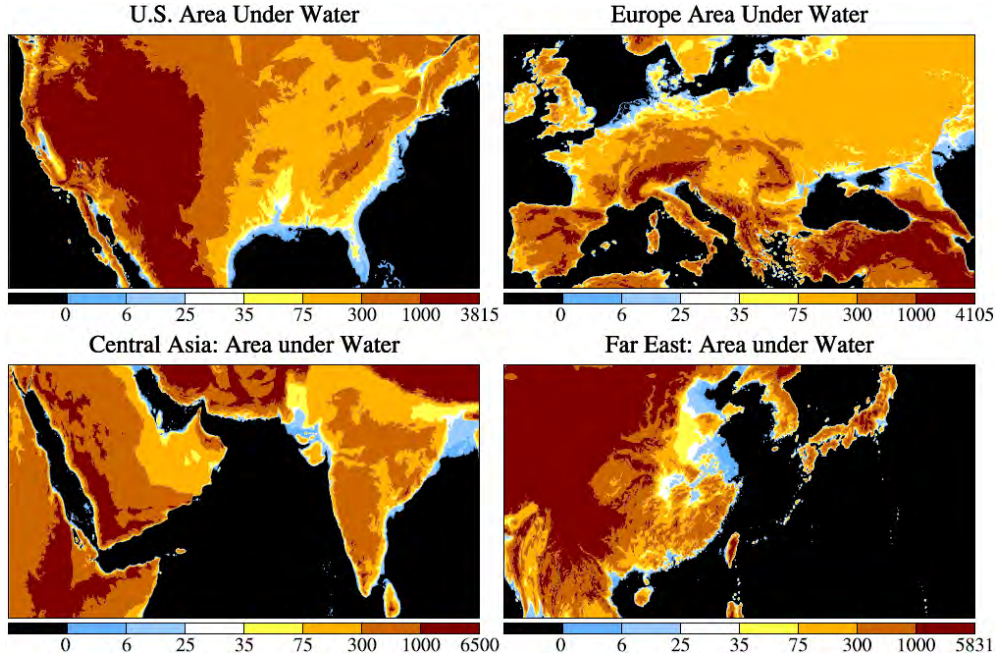

Fig. S23. Areas (light and dark blue) that nominally would be under water for 6 and 25 m sea level rise.

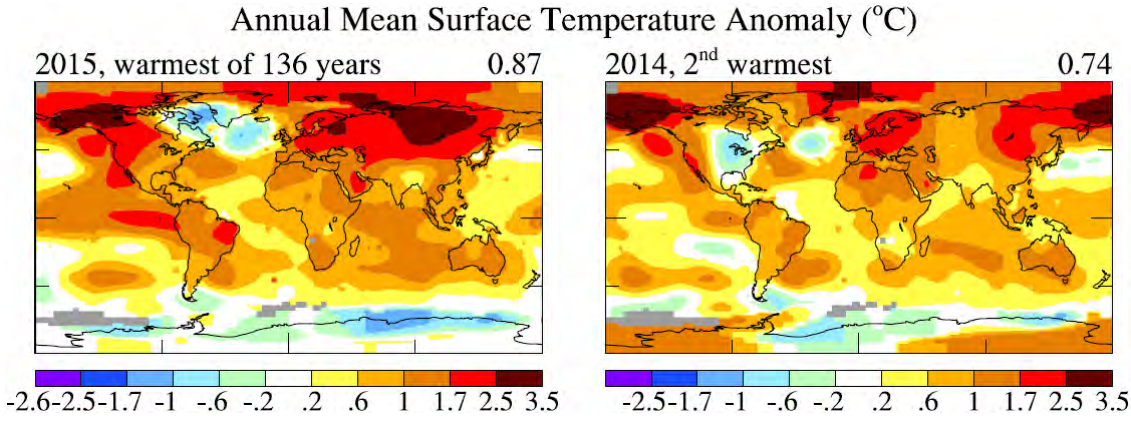

Fig. S24. Observed surface temperature relative to 1951-1980 mean (update of Hansen et al., 2010; maps and other graphs are updated monthly at http://www.columbia.edu/~mhs119/Temperature/).

References for Fig. S1-S24

Boden, T.A., Marland, G., and Andres, R.J.: Global, regional, and national fossil-fuel CO_2 emissions, Carbon Dioxide Information Analysis Center, Oak Ridge National Laboratory, U.S. Department of Energy, Oak Ridge, Tenn., USA, doi 10.3334/CDIAC/00001_V2012, 2012.

Ganachaud, A., and Wunsch, C.: Large-scale ocean heat and freshwater transports during the World Ocean Circulation Experiment, J. Clim., 16, 696-705, 2003.

Seierstad, I.K., Abbott, P.M., Bigler, M., Blunier, T., Bourne, A.J., Brook, E., Buchardt, S.L., Buizert, C., Clausen, H.B., Cook, E., Dahl-Jensen, D., Davies, S.M., Guillevic, M., Johnson, S.J., Pedersen, D.S., Popp, T.J., Rasmussen, S.O., Severinghaus, J.P., Svensson, A., Vinther, B.M.: Consistently dated records from the Greenland GRIP, GISP2 and NGRIP ice cores for the past 104 ka reveal regional millennial-scale $\delta^{18}O$ gradients with possible Heinrich event imprint, Quatern. Sci. Rev., 106, 29-46, 2014.

Supplement S2: Eemian sea level: Evidence for early double peaks and late peak highstand

In Bermuda, Land et al. (1967) were among the first to recognize both a complex Eemian sea level record, and a much higher peak highstand late in the interglacial. Land et al., (1967, Fig. 5 and p.1005) stated: *"Later in the same (MIS 5e) interglacial period the sea rose again, at least to +11 m (east of Spencer's Point)."* Hearty (2002) later surveyed the same Spencer's Point deposits to a more precise +9.2 m ("+" indicates above today's sea level).

In the Mediterranean, a 'double 5e' Eutyrrhenian (Eemian) was a prominent stratigraphic sea level feature described in the 1980s (e.g., Hearty, 1986). Aharon et al. (1980) described a double-5e sea level history from the Papua New Guinea and suggested the higher, late rise was the result of West Antarctic ice collapse. In South Carolina, Hollin and Hearty (1990) similarly documented a double 5e sea level with a rapid late rise several meters higher than the early sea stand. Evidence of a rapid but brief, late rise was further described in Bermuda and the Bahamas in the 1990s (e.g., Hearty and Kindler, 1995). Neumann and Hearty (1996) estimated only a few hundred years to rise to and incise a +6 m notch in the Bahamas. Rapid rise to and brevity at these higher levels is inferred from the prevalence of notches and rubble benches in the Bahamas, in contrast to broad terraces and reefs formed earlier at the +2-3 m level. Additional geological details of these carbonate platform sea level records were contained in a number of interim papers, and summarized in Hearty et al. (2007). Most recently, Godefroid and Kindler (2015) added: *"The MIS 5e record is remarkable. In particular, beach deposits and an intertidal notch at +11 m above msl strongly suggest that sea-level peaked at a much higher elevation than previously assessed, implying pronounced melting of polar ice."*

In the Bahamas, less than 5% of documented Eemian exposures contain coral reefs, and no Eemian *in situ* exposed reefs are known from Bermuda, so U/Th coral dating is not the primary geochronological method available in these areas. Regardless, many of these sparsely distributed reef deposits in the Bahamas have been U/Th dated (e.g., Chen et al., 1991; Hearty et al., 2007; W. Thompson et al., 2011) and correlated with the diagnostic oolites. The geochronological age of Quaternary deposits is based on 275 whole rock and 507 land snail amino acid racemization (AAR) age estimates from U/Th and ^{14}C calibrated age models (Hearty and Kaufman, 2000, 2009). Of key importance, the Eemian-MIS 5e in the Bahamas is defined by its position in the stratigraphic sequence of the rocks, the oolitic and pristine aragonitic sedimentology, a unique landsnail fauna (Garrett and Gould, 1984), and numerous additional diagnostic characteristics (e.g., Hearty and Neumann, 2001, p. 1883). There is little disagreement among researchers of the defining characteristics of MIS 5e in the Bahamas.

What gives carbonate platforms such as Bermuda and the Bahamas the unique quality of preserving such a detailed geologic record? Because carbonate sediments, particularly ooids, respond and cement quickly, the highly mobile sediments that mantle flat-topped carbonate platforms effectively record and preserve rock evidence of short-lived energetic events such as storms and rapid sea level changes. Corals and coral reefs respond too slowly and cannot record such brief changes. Likewise, similar short-term events are not preserved on coasts dominated by siliciclastic or volcanic sediments (e.g., US East Coast and much of Caribbean region) due to the instability and slowness of cementation ($>10^6$ yr) of non-carbonate sediments.

In a global multidisciplinary review of MIS 5e, Hearty et al. (2007) assembled shoreline stratigraphy, field information, and geochronological data from 15 sites to construct a composite curve of Eemian sea level change. Their reconstruction has sea level rising in the early Eemian to +2-3 m. Mid-Eemian sea level may have fallen a few meters to a level near today's sea level.

Sea level then rose rapidly in the late Eemian to +6-9 m, cutting multiple bioerosional notches in older limestone in the Bahamas and elsewhere.

Along the northeast Yucatan Peninsula, Mexico, Blanchon et al. (2009) used a sequence of coral reef crests to investigate coral reef "back-stepping", i.e., the fact that coral reef building moves shoreward as sea level rises with a higher temporal precision than possible with U-series dating alone. They documented an early +3 m sea level jump by 2-3 m to +6 m within an "ecological" period, i.e., within several decades, in the late Eemian about 121 ky b2k based on U/Th ages. W. Thompson et al. (2011) reexamined the Eemian using corrected U-series coral reef data from the Bahamas and interpreted a mid-Eemian sea level at +4 m at 123 ky b2k, a maximum at +6 m at 119 ky b2k, and at 0 m at some time in between. Note that no known coral reef crests are higher than +2-3 m across the entire archipelago (Hearty and Neumann, 2001; p. 1883).

In Western Australia, O'Leary et al. (2013) assembled one of the most comprehensive Eemian sea level studies that includes: 1) 28 "far field" study sites along the 1400 km coastline; 2) application of a multi-disciplinary approach using geomorphology, stratigraphy, and sedimentology; 3) high-precision U/Th dating and screening of over 100 in situ corals; and 4) incorporation of GIA correction regionally yielding a more precise eustatic sea level history. The O'Leary et al. (2013) analyses suggest that sea level was relatively stable at 3-4 m in most of the early-mid Eemian, followed by a brief but rapid (<1000 yr) late-Eemian sea level rise to about +9 m. U-series dating of the corals has the sea level rise begin at 119 ky b2k and peak sea level at 118.1 ± 1.4 ky b2k.

The far field *eustatic* sea level changes documented across Western Australia (O'Leary et al., 2013) agree closely with the relative sea level shifts from near and mid field Bermuda and the Bahamas (Hearty et al., 2007). Nearly all global sites in the Hearty et al. (2007) study showed the same *relative* changes: early prolonged stability, a minor mid regression, then finally rapid upward shifts of 3 to 5 m late in the Eemian. Such rapid sea level changes require ice sheet growth and melting, regional glacio-isostatic adjustment (GIA), or both.

Additional References (others are in the main text)

Aharon, P., Chappell, J., and Compston, W.: Stable isotope and sea level data from New Guinea supports Antarctic ice-surge theory of ice ages. Nature, 283, 649-651, 1980.

Garrett, P. and Gould, S.J.: Geology of New Providence Island, Bahamas. Geological Society of America Bulletin 95, 209–220, 1984.

Godefroid, F., and Kindler, P. Prominent geological features of Crooked Island, SE Bahamas. The 16th Symposium on the Geology of the Bahamas and other Carbonate Regions. P. 26-38. 2015.

Hearty, P.J.: An inventory of last interglacial (s.1) age deposits from the Mediterrnean basin: a study of isoleucine epimerization and U-series dating. Zeitschrift fur Geomorphologie 62 (Suppl.), 51,-69, 1986.

Hearty, P.J.: A revision of the late Pleistocene stratigraphy of Bermuda. Sedimentary Geology 153 (1-2) 1-21, 2002.

Hearty, P.J. and Kaufman, D.S.: Whole-rock aminostratigraphy and Quaternary sea-level history of the Bahamas. Quaternary Research 54, 163–173, 2000.

Hearty, P.J. and Kaufman, D.S., 2009. A high-resolution chronostratigraphy for the central Bahama Islands based on AMS ^{14}C ages and amino acid ratios in whole-rock and Cerion land snails. Quaternary Geochronology 4, 148-159. 1995.

Hearty, P.J. and Kindler, P.: Sea-level highstand chronology from stable carbonate platforms (Bermuda and the Bahamas). In: Davis, R.A., Donoghue, J.F., and Krantz, D.E., (eds.) Episodic Sea-level Change. Journal of Coastal Research 11(3): 675-689, 1995.

Hearty, P.J., Neumann, A.C., and O'Leary, M.J.: Comment on "Record of MIS 5 sea-level highstands based on U/Th dated coral terraces of Haiti" (B. Dumas, C.T. Hoang, and J. Raffy, 2006, Quaternary International, v. 145-146, p. 106-118). Quaternary International, v. 162-163, p. 205-208, 2007.

Hollin, J.T., and Hearty, P.J.: South Carolina Interglacial sites and Stage 5 sea levels. Quaternary Research 33: 1-17, 1990.

Supplement S3: Ocean wave splash near the location of Eleuthera boulders

Cox et al. (2012) discuss the inadequacy of hydrodynamic modeling to realistically describe movement of boulders by large storms. Specifically, they found that storms in the North Atlantic had thrown boulders as large as 80 tons to a height 11 m AHWM (above high water mark) on the shore on Ireland's Aran Islands, the specific storm on 5 January 1991 being driven by a low pressure system that recorded a minimum 946 mb (equivalent to a category 3 hurricane). Winds gusted to 80 knots and the closest weather station to the Aran Islands recorded gale force winds for 23 hours and sustained winds of 40 knots for five hours. The storm waves built on swell previously developed by strong winds during the prior two weeks.

Cox et al. (2012) note that existing hydrodynamic modeling equations would not lift the boulders, and they cite two reasons to disregard those equations. First, they note that wave height measurements frequently reveal waves twice the SWH (significant wave height) of wave models. Second, existing wave equations do not include the effects of reflection from cliff and shoreline, and the attendant wave amplification. Cox et al. note that wave heights at shoreline cliffs can be much greater than the equilibrium height of approaching deep-water waves. The waves steepen as they shoal, impact the coast, reflect back, meet advancing wave crests causing a mixture of constructive and destructive interference, with intermittent production of very large individual waves capable of quarrying and transporting large blocks and boulders.

These considerations help explain why megaboulders (as large as ~1000 tons) on Eleuthera are only found just south of the Glass Window Bridge at the apex of an embayment that funnels the waves before they encounter a steep shoreline cliff (Figs. 1-3 of Hearty, 1998; see also Hearty, 1997). The special effect of the location and shoreline cliff is shown in a photo (Fig. 1). Despite relatively calm conditions on Eleuthera, as indicated by the waters in the photo, immediately southwest of the narrow Eleuthera island, the northeast side of Eleuthera was being battered by large waves generated in the North Atlantic by the 1991 "Perfect Storm". The Perfect Storm originated as an extratropical low east of Nova Scotia that tracked first toward the southeast and then west, sweeping up remnants of Hurricane Grace, which deepened the low. The storm eventually reached a peak intensity with sustained winds of 75 mph (120 km/h), a category 1 hurricane, making landfall on Nova Scotia on 2 November. The shoreline cliffs immediately south of the Glass Window Bridge, facing slightly east of due north (Fig. 3 Hearty, 1998), were battered by the deep long-period waves generated by the storm in the North Atlantic.

Irregularity of ocean spash in this setting probably helps account for how an unsuspecting bread truck driver, seduced by the relative calm and fair weather (Fig. 1), was swept off the road by one of the bursts as water swept across the road. The truck was thrown/washed well into the shallow waters on the Caribbean-facing side of the island – the driver escaped in these relatively calm waters to the southwest, but his rusted out truck frame remains there today.

Further confirmation of the ability of storm waves to lift large boulders was provided recently by May et al. (2015). Despite the fact that this storm did not have the "advantage" of being stationary for the long period required to develop deep powerful waves, the typoon produced longshore transport of a 180 ton block and lifted boulders of up to ~24 tons to elevations as high as 10 m. May et al. (2015) conclude that these observed facts "…demand a careful re-evaluation of storm-related transport where it, based on the boulder's sheer size, has previously been ascribed to tsunamis."

Additional References (others are in the main text)

Hearty, P.J.: The geology of Eleuthera Island, Bahamas: A rosetta stone of Quaternary stratigraphy and sea-level history, Quatern. Sci. Rev., 17, 333-355, 1998.

Photograph S1. Photo taken 31 October 1991 from a few hundred meters offshore of the southern protected bank-side at the narrow part of Eleuthera near the Glass Window Bridge, looking northeast (Tormey, 1999; see text). The telephone pole on the left and the 15-20 m cliff provide scale.